Progress In Electromagnetics Research, Vol. 162, 39–50, 2018

Exploiting the Topological Robustness of Composite Vortices in Radiation Systems

Mirko Barbuto[1, *], Mohammad-Ali Miri[2], Andrea Alù[2], Filiberto Bilotti[3], and Alessandro Toscano[3]

Abstract—Recent years have witnessed an increasing interest in topological states of condensed matter systems, whose concepts have been also extended to wave phenomena. Especially at optical frequencies, several studies have reported applications of structured light exploiting topological transitions and exceptional points or lines, over which a field property of choice is undefined. Interesting properties of light beams with phase singularities (such as the creation, annihilation or motion of these topological points) have been observed in composite vortices consisting of superimposed light beams with different topological charges. Here, we discuss how these concepts may have a relevant impact on antenna technology at microwave frequencies. We obtain the superposition of vortex fields with different topological charges by simultaneously exciting different modes of a patch antenna. This can be useful to give a physical interpretation for the behavior of some structures, already proposed at microwave frequencies, which use superposition of different radiating modes to manipulate the radiation pattern of patch antennas. Moreover, this approach may open new strategies to design at will the directivity properties of a patch antenna with inherently robust responses, and it may find applications in the design of smart antenna systems, requiring pattern reconfigurability.

1. INTRODUCTION

Structured light is a research topic of broad and current interest in optics, referring to the generation and application of customized electromagnetic fields with tailored polarization, amplitude and/or phase [1]. Although several classes of structured fields have been theoretically predicted and experimentally realized, this term is often used in relation to the more specific topic of optical vortices (OV) or Orbital Angular Momentum (OAM). As originally pointed out by Nye and Berry, vortices are singularities where phase is undefined, thus the intensity is inevitably zero [2]. In general, such phase singularities are associated with a discrete topological charge, rendering them robust with respect to small perturbations [3]. At optical frequencies, vortex beams have found numerous applications, among which 3D manipulation of microscopic particles [4], advanced imaging systems [5], classical or quantum communications [6]. Moreover, linear and nonlinear properties of structured light have been deeply investigated [7–10]. Recently, the generation of structured fields has been extended to microwave frequencies [11], but practical applications in this frequency range are still at their early stages. In particular, what at first seemed to be the most promising, i.e., the possibility of exploiting the orthogonality between different OAM modes to increase the channel capacity of a communication system, turned out to be only a specific, sub-optimal case of a MIMO system, a rich field of research which appears well more advanced than the OAM specific scenario [12].

Received 30 March 2018, Accepted 30 April 2018, Scheduled 28 May 2018
* Corresponding author: Mirko Barbuto (mirko.barbuto@unicusano.it).
[1] "Niccolò Cusano" University, Rome 00166, Italy. [2] Department of Electrical and Computer Engineering, University of Texas at Austin, Austin, TX 78701, USA. [3] Engineering Department, "Roma Tre" University, Rome 00146, Italy.

Nevertheless, in recent years, several radiating systems have been proposed to generate microwave fields with OAM, exploiting antenna arrays with proper element excitation phasing [13, 14], mechanically modified parabolic or spiral reflectors [15, 16], metasurfaces [17], ring antennas [18], spiral phase plate [19], spiral antennas [20], or patch antennas working with circularly polarized (CP) higher-order modes [21], just to cite a few. In particular, we have shown that the higher-order TM_{nm} modes of a circularly polarized patch antenna radiate an electromagnetic field with OAM distribution of order $\pm(n-1)$, where the plus/minus sign indicates a right- or left-handed polarization, respectively. We have also shown that a more complex structured field, characterized by a polarization state that resembles the structure of a Mobius strip, can be generated at microwaves using a similar approach [22]. This peculiar topological structure was first observed at optical frequencies [23] and, as in our investigation, results from the proper superposition of different fields with topological singularities. To the best of our knowledge, the direct investigation at microwave frequencies of the superposition of two electromagnetic fields, at least one of which exhibiting phase singularities, is limited to the aforementioned scenario generating a Mobius polarization state. On the contrary, at optical frequencies, several works have extensively discussed the properties of composite vortices consisting of beams with different topological charges. One of the main reasons is that phase singularities are structurally stable features of fields, which may be found even if the vortex beam is highly perturbed. Therefore, several groups have studied the conditions for obtaining translation, creation or annihilation of phase singularities when different OV are superimposed (see, for instance [24–26]).

In this paper, inspired by the aforementioned works, we explore the generation of composite vortices at microwave frequencies and investigate the possibilities offered by the superposition of topological singularities in antenna systems. In particular, the structure of the manuscript is as follows: in Section 2, we show that, by properly superimposing two different radiating modes of a patch antenna, one of which exhibiting a phase singularity, we can change the location of this singularity and, thus, directly shape or rotate the radiation pattern of the radiating element. More specifically, by varying the excitation amplitude of the two modes, one can change the shape of the radiation pattern, while by varying the relative phase shift one can rotate the radiation pattern at will. Then, in Section 3, we numerically validate our results, and finally, in Section 4, we draw the conclusions.

2. ANALYTICAL STUDY OF COMPOSITE VORTICES GENERATED BY A CIRCULAR PATCH ANTENNA

In a recent paper by our group [21], it has been demonstrated that the higher-order modes of a circular patch antenna, if circularly polarized, are characterized by phase vortices and amplitude nulls, which can be exploited to radiate an electromagnetic field with OAM. Inspired by an experimental work performed at optical frequencies [23], we have combined one of these higher-order modes with the fundamental one to obtain particular spatial distributions of both amplitude and phase. In particular, by an appropriate choice of the modes and their polarizations, a Mobius polarization state for the radiated field has been obtained [22]. However, this is only one of the numerous structured fields that can be generated by using composite vortices generated by standard radiating systems.

In fact, as already demonstrated in optics, the superposition of vortex beams can generate a wide variety of topological structures of phase and intensity, such as loops, links and knots in 3D space [27], or interesting polarization topologies [28, 29]. Moreover, phase singularities of vortex beams have a topological nature and, thus, are robust to a large range of external perturbations. Therefore, by adding a constant background to a vortex beam, the phase singularities do not completely disappear but only translate to another point of zero intensity [3]. For the same reason, if we add two vortex beams, the number and location of the vortices in the total field directly depend on the charge of the constituting beams and their relative phase and amplitude. In particular, as demonstrated in [24], the collinear superposition of two vortices with different order (n_1 and n_2, with $n_2 > n_1$) results in a vortex of order n_1 in the origin and $|n_2 - n_1|$ vortices of charge $n_2/|n_2|$ placed at a distance r from the origin and rotated by an angle Φ, where:

$$\Phi = \frac{\delta + n\pi}{n_2 - n_1} \tag{1}$$

and

$$r = \frac{w}{\sqrt{2}} \left(\sqrt{\frac{|n_2|!}{|n_1|!}} \tan \alpha \right)^{1/(|n_2|-|n_1|)} \tag{2}$$

being w the beam radius and n an odd integer, while α and δ specify the relative amplitude and phase of the two beams, respectively.

In order to obtain similar phenomena at microwave frequencies, we consider here the case of a circular patch antenna simultaneously supporting its fundamental mode (TM_{11}) and the first higher-order mode (TM_{21}), both working under right-handed circular polarization (RHCP) at the same operating frequency. For the sake of clarity, we start considering the field radiated by a generic TM_{nm} mode for linear polarization, which has been derived by using the cavity model in cylindrical coordinates and is given by [30]:

$$\begin{aligned} E_{\theta n} &= j^n \frac{V_n k_0 a_n}{2} \frac{e^{-jk_0 r}}{r} \cos n\varphi \left[J_{n+1}(\gamma) - J_{n-1}(\gamma) \right] \\ E_{\varphi n} &= j^n \frac{V_n k_0 a_n}{2} \frac{e^{-jk_0 r}}{r} \cos\theta \sin n\varphi \left[J_{n+1}(\gamma) + J_{n-1}(\gamma) \right] \end{aligned} \tag{3}$$

where, r, θ, and φ are the polar coordinates; $V_n = hE_0 J_n(ka_n)$ is the edge voltage at $\varphi = 0$; h is the thickness of the dielectric substrate; E_0 is the value of the electric field at the edge of the patch; $\gamma_n = k_0 a_n \sin\theta$, a_n is the radius of the patch; J_i is the Bessel function of the first kind and order i, k and k_0 are the propagation constants in the dielectric and free space, respectively. Since a requirement for obtaining a phase singularity in patch antennas is the use of circular polarized modes [21], we have to generalize these expressions to a CP TM_{nm} mode. For this purpose, we can consider that circular polarization can be obtained using two coaxial feeds with proper angular spacing with respect to each other, such that two orthogonal linearly polarized modes with a proper phase shift are excited. Therefore, considering the circular polarization as a superposition of the individual electric fields produced by two linearly polarized orthogonal modes, the total radiated field by a CP TM_{nm} mode can be expressed as [31]:

$$\begin{aligned} E^t_{\theta n} &= E^1_{\theta n}(\phi, \theta) + jE^2_{\theta n}(\phi + \tau, \theta) \\ E^t_{\varphi n} &= E^1_{\varphi n}(\phi, \theta) + jE^2_{\varphi n}(\phi + \tau, \theta) \end{aligned} \tag{4}$$

where superscripts 1 and 2 correspond to the fields generated by the two orthogonal modes, respectively; τ is the angular spacing of the feeds depending on the mode order [31]; the phase shift between the two modes has been chosen equal to $\pi/2$ in order to obtain a RHCP field.

These expressions can now be used to derive the overall radiated field, which can be considered as the weighted sum of the fields radiated by the RHCP TM_{11} and the RHCP TM_{21} modes:

$$\begin{aligned} E^t_\theta &= \sin(\alpha) \left[E^1_{\theta 1}(\phi, \theta) + jE^2_{\theta 1}(\phi + \tau, \theta) \right] + \cos(\alpha) \left[E^1_{\theta 2}(\phi, \theta) + jE^2_{\theta 2}(\phi + \tau, \theta) \right] e^{j\delta} \\ E^t_\varphi &= \sin(\alpha) \left[E^1_{\varphi 1}(\phi, \theta) + jE^2_{\varphi 1}(\phi + \tau, \theta) \right] + \cos(\alpha) \left[E^1_{\varphi 2}(\phi, \theta) + jE^2_{\varphi 2}(\phi + \tau, \theta) \right] e^{j\delta} \end{aligned} \tag{5}$$

where, again, α and δ specify the relative amplitude and phase of the two components, respectively.

Given that only TM_{21} mode is characterized by a phase singularity, the expressions in Eq. (5) consists of a constant background (the RHCP TM_{11} mode) superimposed to a vortex beam (the RHCP TM_{21} mode). Therefore, depending on α and δ, the position of the phase singularity and, thus, of the amplitude null, is expected to vary with respect to the original one, i.e., to the propagation axis. Moreover, in [21] we have shown that in Cartesian coordinates relations in Eq. (4) can be simplified to:

$$\begin{aligned} E_{xn} &= A_n e^{-j(n-1)\phi} - B_n e^{-j(n+1)\phi} \\ jE_{yn} &= A_n e^{-j(n-1)\phi} + B_n e^{-j(n+1)\phi} \end{aligned} \tag{6}$$

with amplitudes:

$$\begin{aligned} A_n &= -j^n \frac{V_n k_0 a_n}{2} \frac{e^{-jk_0 r}}{r} \cos\theta J_{n-1}(\gamma_n) \\ B_n &= -j^n \frac{V_n k_0 a_n}{2} \frac{e^{-jk_0 r}}{r} \cos\theta J_{n+1}(\gamma_n) \end{aligned} \tag{7}$$

Therefore, the total field of Eqs. (5) reduce to:

$$\begin{aligned} E_x &= \sin\alpha\left(A_1 - B_1 e^{-j2\phi}\right) + e^{j\delta}\cos\alpha\left(A_2 e^{-j\phi} - B_2 e^{-j3\phi}\right) \\ jE_y &= \sin\alpha\left(A_1 + jB_1 e^{-j2\phi}\right) + e^{j\delta}\cos\alpha\left(A_2 e^{-j\phi} + jB_2 e^{-j3\phi}\right) \end{aligned} \tag{8}$$

Using Eq. (7) in Eq. (8) we obtain:

$$\begin{aligned} \left(\frac{k_0}{2}\frac{e^{-jk_0 r}}{r}\right)^{-1} E_x = &- jV_1 a_1 \sin\alpha\left(J_0(\gamma_1) - J_2(\gamma_1)\, e^{-j2\phi}\right)\cos\theta \\ &+ e^{j\delta} V_2 a_2 \cos\alpha\left(J_1(\gamma_2)\, e^{-j\phi} - J_3(\gamma_2)\, e^{-j3\phi}\right)\cos\theta \\ j\left(\frac{k_0}{2}\frac{e^{-jk_0 r}}{r}\right)^{-1} E_y = &- jV_1 a_1 \sin\alpha\left(J_0(\gamma_1) + J_2(\gamma_1)\, e^{-j2\phi}\right)\cos\theta \\ &+ e^{j\delta} V_2 a_2 \cos\alpha\left(J_1(\gamma_2)\, e^{-j\phi} + J_3(\gamma_2)\, e^{-j3\phi}\right)\cos\theta \end{aligned} \tag{9}$$

Limiting our attention to small deviations from the propagation axis z, we consider $\gamma_n = k_0 a_n \sin\theta \ll 1$, thus in each bracket one of the Bessel functions can be neglected in compared to the other one, i.e., $J_0(\gamma_1) \gg J_2(\gamma_1)$ and $J_1(\gamma_2) \gg J_3(\gamma_2)$, which in turns results in the simplified relations:

$$\begin{aligned} \left(\frac{k_0}{2}\frac{e^{-jk_0 r}}{r}\right)^{-1} E_x &= -jV_1 a_1 \sin\alpha J_0(\gamma_1)\cos\theta + e^{j\delta} V_2 a_2 \cos\alpha J_1(\gamma_2)\, e^{-j\phi}\cos\theta \\ j\left(\frac{k_0}{2}\frac{e^{-jk_0 r}}{r}\right)^{-1} E_y &= -jV_1 a_1 \sin\alpha J_0(\gamma_1)\cos\theta + e^{j\delta} V_2 a_2 \cos\alpha J_1(\gamma_2)\, e^{-j\phi}\cos\theta \end{aligned} \tag{10}$$

Therefore, under this approximation, the field components can simultaneously vanish at:

$$-jV_1 a_1 \sin\alpha J_0(\gamma_1) + e^{j\delta} V_2 a_2 \cos\alpha e^{-j\phi} J_1(\gamma_2) = 0 \tag{11}$$

Considering again $\gamma_n \ll 1$, one can write $J_0(\gamma_1) \approx 1$ and $J_1(\gamma_2) \approx \frac{\gamma_2}{2}$, therefore:

$$-j\sin\alpha + \frac{V_2}{V_1} e^{j(\delta-\phi)}\cos\alpha \frac{k_0 a_2^2}{2a_1}\sin\theta = 0 \tag{12}$$

which results in a simple expression for the phase singularity point:

$$\begin{aligned} \phi &= \delta - \frac{\pi}{2} \\ \sin\theta &= \frac{2a_1}{k_0 a_2^2}\frac{V_1}{V_2}\tan\alpha \end{aligned} \tag{13}$$

According to these relations, on a given z-plane in the far field, the distance of the vortex from the origin depends on α while its azimuth depends only on δ. In particular, for $\delta = 0$, the singularity is on the negative y-axis and by increasing α it moves away from the center. For a fixed value of α, instead, by increasing δ the vortex rotates around a fixed circle.

In order to validate these results, we have analyzed the amplitude and phase patterns of the overall radiated field on a plane orthogonal to the propagation direction at a distance λ_0 (being λ_0 the operating wavelength in free space) from the patch, for different values of α and δ. The results are summarized in the next subsections.

2.1. Effects of Varying α

In Fig. 1, we show the phase patterns of the x- and y-components of the radiated field assuming $\delta = 0$ and for different values of α. This parameter, being the argument of the two basic trigonometric functions in (5), specifies the relative amplitude of the two modes. Therefore, the two limiting cases will be $\alpha = 0$, corresponding to the presence of the TM_{21} mode only, and $\alpha = \pi/2$, corresponding to presence of the TM_{11} mode only. In particular, in the first case, there is a phase singularity in the center

beam. On the contrary, in the second case, the radiated field has no phase singularity. For $0 < \alpha < \pi/2$, the field with no phase singularity cannot suppress the topological charge of the higher-order mode, but the corresponding phase singularity moves away from the center beam, due to the superposition with a constant background. These results confirm that, by acting on α, i.e. on the excitation amplitudes of the two modes, it is possible to move the phase vortex present on the Cartesian components of the radiated field. Moreover, as a phase singularity point is intrinsically connected to an amplitude null, by varying α also the dark core of the radiated field can be moved away from the center of the radiating structure. This is confirmed by Fig. 2, which shows the amplitude patterns of the radiated field for different values of α. Overall, these results confirm the inherent robustness of the proposed mechanism to control and reconfigure the radiation of these antenna elements, inherently associated with their topological properties.

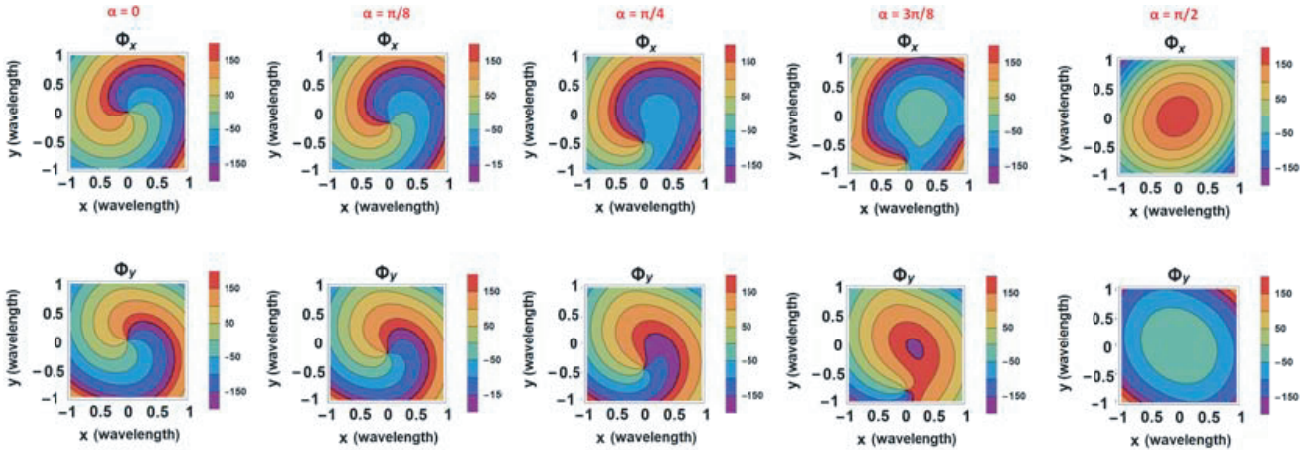

Figure 1. Analytically calculated phase (Φ_x and Φ_y) distributions (in degree) at a distance λ_0 from the patch of the electric field radiated by the superposition of RHCP TM_{11} and RHCP TM_{21} modes for different values of α (here $\delta = 0$).

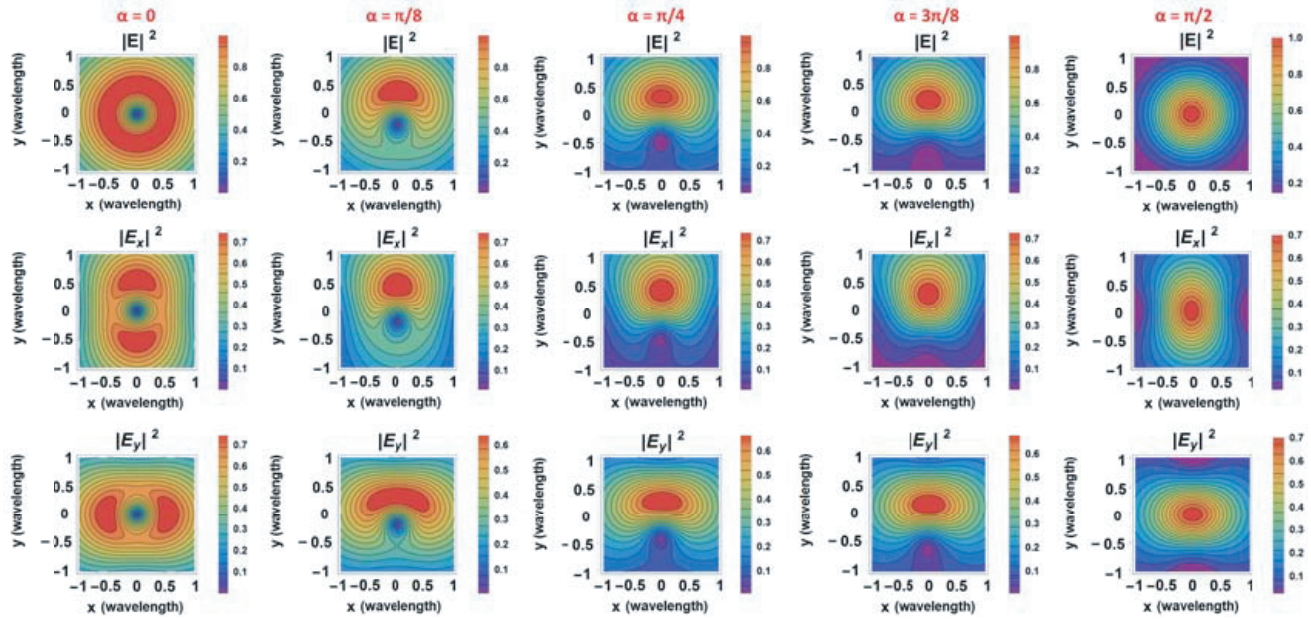

Figure 2. Analytically calculated total electric energy density ($|E|^2$) and amplitude ($|E_x|^2$ and $|E_y|^2$) distributions of the electric field radiated by the superposition of RHCP TM_{11} and RHCP TM_{21} modes for different values of α.

2.2. Effects of Varying δ

As demonstrated in [24], by varying the phase difference between two vortex fields, one can rotate the resulting vortices around the center beam. In order to demonstrate this effect at microwave frequencies, we focus our attention, without loss of generality, on the case $\alpha = \pi/4$ (the RHCP TM_{11} mode and the RHCP TM_{21} mode are excited with equal amplitude). We analyze the phase patterns of the x- and y-component of the radiated field for different values of δ, reported in Fig. 3. From this figure, we can see that the topological singularity of the RHCP TM_{21} mode is always present, but it rotates around the center beam, being the rotation angle proportional to the phase angle δ, as predicted by (13). The same phenomenon occurs for the amplitude null, as shown in Fig. 4, which rigidly rotates with the phase singularity. Again, the presence of the topological charge is very robust in the radiation patterns, and its position can be controlled with large flexibility by tailoring the relative phases of the excited modes.

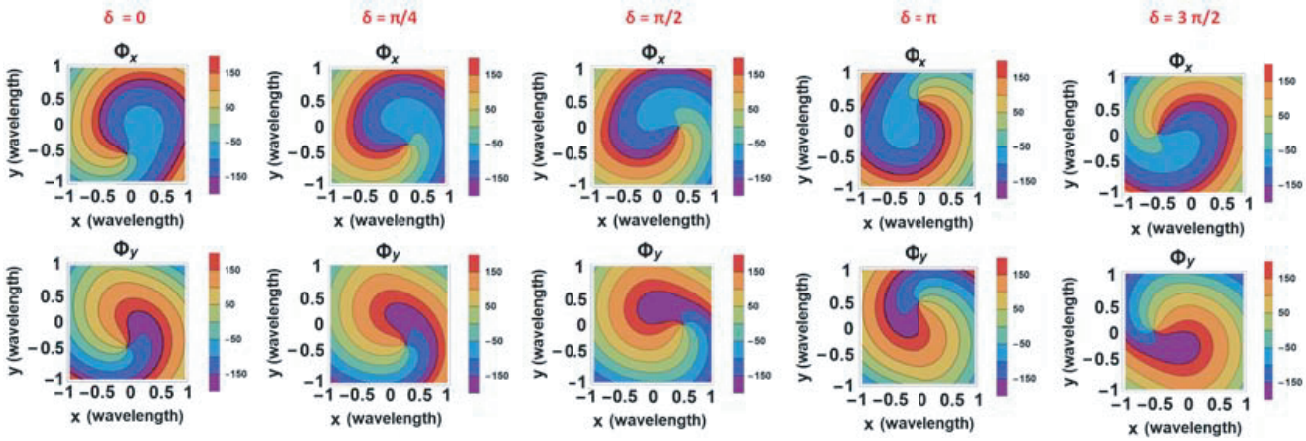

Figure 3. Analytically calculated phase (Φ_x and Φ_y) distributions (in degree) of the electric field radiated by the superposition of RHCP TM_{11} and RHCP TM_{21} modes for different values of δ (here $\alpha = \frac{\pi}{4}$).

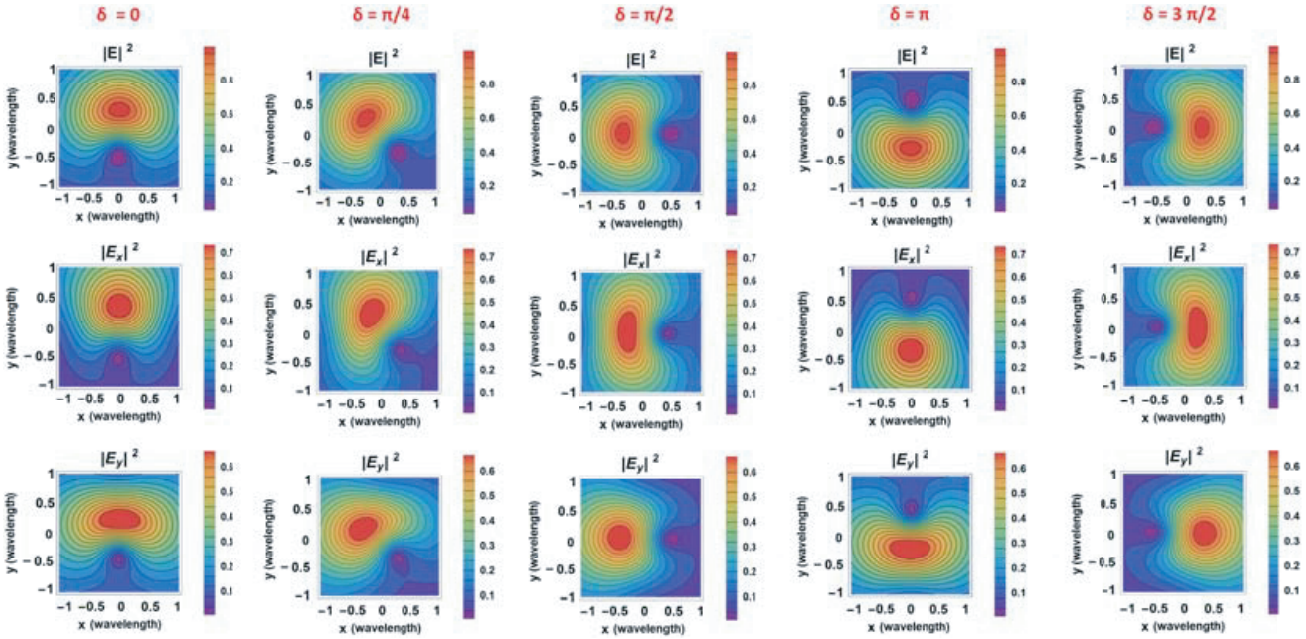

Figure 4. Analytically calculated total electric energy density ($|E|^2$) and amplitude ($|E_x|^2$ and $|E_y|^2$) distributions of the electric field radiated by the superposition of RHCP TM_{11} and RHCP TM_{21} modes for different values of δ.

2.3. Effects on the Radiation Patterns

The previous analysis extends the concept of composite vortices to microwave antennas, and it provides a simple method to superimpose electromagnetic fields with different topological charge, based on the use of standard radiating systems. This may be useful to create test benches at much lower frequencies than those typically used in this research field, or for investigating if the application of optical composite vortices can be extended to a lower frequency range, for instance for wireless communications. Moreover, the superposition of topological singularities of vortex beams has also a direct application in antenna technology. In this context, we stress here that for antenna engineers a key variable to describe the antenna response is the radiation pattern, which defines the variation of the radiated power by an antenna as a function of the direction away from the antenna itself. Since the radiation pattern is directly related to the electromagnetic field radiated by the antenna, we expect that the effects on the radiated field observed in the previous subsection will be also reflected on the shape and orientation of the radiation pattern. To demonstrate this statement, starting from (5), we have evaluated the 3D directivity of the patch antenna for different values of α and δ. At first, we have analyzed the effect of α on the shape of the radiation pattern and reported in Fig. 5 the main results. As expected, for $\alpha = 0$, the antenna radiates with the typical conical pattern of a patch antenna working on the higher-order TM_{21} mode [31]. On the contrary, for $\alpha = \pi/2$, the radiation pattern has a maximum in the broadside direction, as expected for a patch antenna working on the fundamental TM_{11} mode. By increasing α from 0 to $\pi/4$, the shape of the radiation pattern gradually narrows and the maximum directivity increases; while going beyond $\pi/4$ the maximum pointing angle of the radiation pattern increases until it reaches the broadside direction. Then, in order to evaluate the effect of varying δ, we have focused again, without loss of generality, on the case with $\alpha = \pi/4$ and reported in Fig. 6 the corresponding radiation patterns for different values of δ. From this figure, it is evident that, by adding a phase shift between the two exciting modes, the radiation pattern rotates around the vertical axis of the same amount.

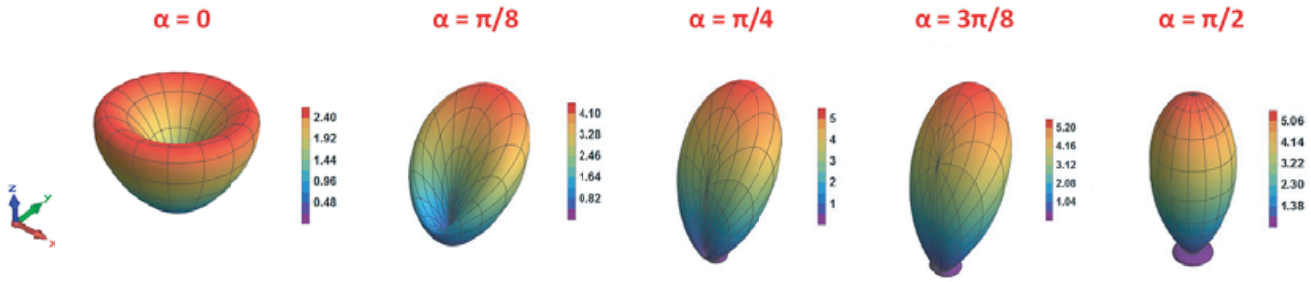

Figure 5. Analytically calculated directivity patterns (expressed in dB) of the patch antenna supporting the superposition of RHCP TM_{11} and RHCP TM_{21} modes for different values of α.

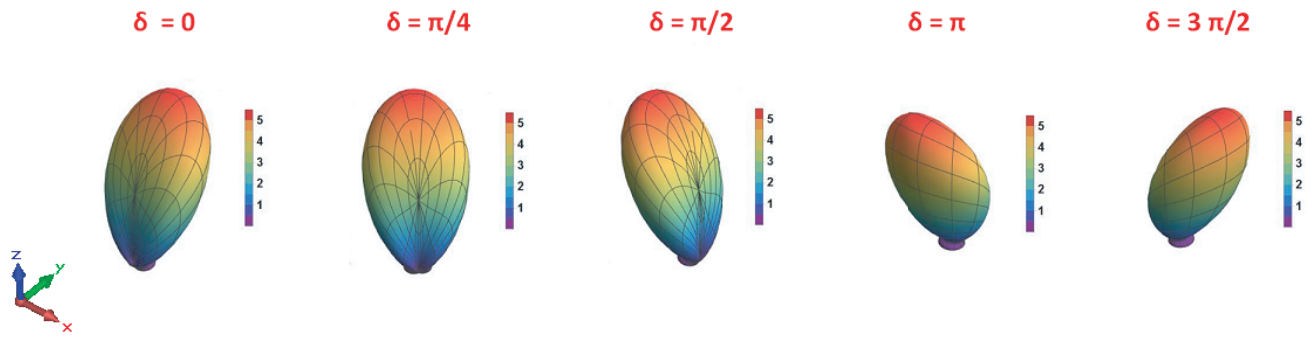

Figure 6. Analytically calculated directivity patterns (expressed in dB) of the patch antenna supporting the superposition of RHCP TM_{11} and RHCP TM_{21} modes for different values of δ.

3. FULL-WAVE NUMERICAL VALIDATION

In this section, we validate the accuracy of the analytical results reported in the previous Section by performing a set of numerical simulations. Moreover, we describe the design procedure to obtain a realistic radiating element able to radiate, at the same frequency and simultaneously, two electromagnetic fields with different topological charges. As discussed in [22], the TM_{nm} modes supported by a radiating circular metallic patch have different operating frequencies. Consequently, the composite vortices cannot be directly generated by using a single patch antenna. A possible solution, already used in [22] to generate a Mobius polarization state, is to design a single structure consisting of two radiating elements concentrically placed. In this way, the different dimensions of the two radiating elements can be properly designed to support two different resonant modes, i.e., the TM_{11} and the TM_{21} mode in our analysis, at the same operating frequency. In order to generate the two radiating modes with circular polarization, the radiating elements should present a proper geometrical asymmetry so that, for each of them, two degenerate modes are excited with a 90° phase shift between them. A possible structure that takes into account all these design constraints is shown in Fig. 7. It consists of an inner metallic patch and an external metallic ring, both placed on a grounded dielectric substrate (Roger Duroid^{TM} RT5870, $\varepsilon_r = 2.33$, $\tan\delta = 0.0012$ and thickness 0.787 mm). Both elements are excited with their own coaxial feed (indicted with p_1 and p_2 in Fig. 7), whose position has been determined to excite, with equal amplitude, the corresponding degenerate modes. Moreover, the external element is connected to the metallic ground through a metallic strip, in order to achieve good impedance matching. The square slits placed on the boundary of the two radiating elements have instead the required geometrical asymmetry for circular polarization operation. Please note that, contrary to [22], in the structure here proposed the two coaxial feeds are placed on the same side respect to the yz-plane, in order to obtain two circular polarized modes with the same handedness.

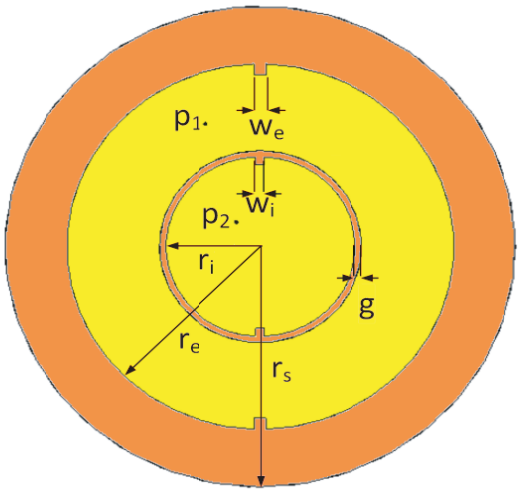

Figure 7. Geometrical sketch of the proposed radiating structure. Dimensions: $g = 2.1$ mm, $r_e = 38.5$ mm, $r_i = 18.5$ mm, $r_s = 49.9$ mm, $w_e = 2.33$ mm, $w_i = 1.85$ mm.

In order to evaluate the response of the proposed structure, a set of full-wave numerical simulations has been performed with the commercial package CST Studio Suite. For the sake of brevity, we report here the analysis for the exciting configuration: $\alpha = \pi/4$ and $\delta = 0$; while for the other excitation we show only the corresponding radiation pattern. The performance of the overall structure has been evaluated when the two radiating elements are simultaneously excited with the same signal amplitude and phase using an ideal 3 dB power divider. In this case, as shown in Figs. 8 and 9, the antenna has a good impedance matching and it radiates a circularly polarized field with good polarization purity around the operating frequency of 3 GHz. We have performed a 3D-electromagentic/circuit co-simulation to evaluate the amplitude and phase patterns of the total radiated fields, reported in Fig. 10.

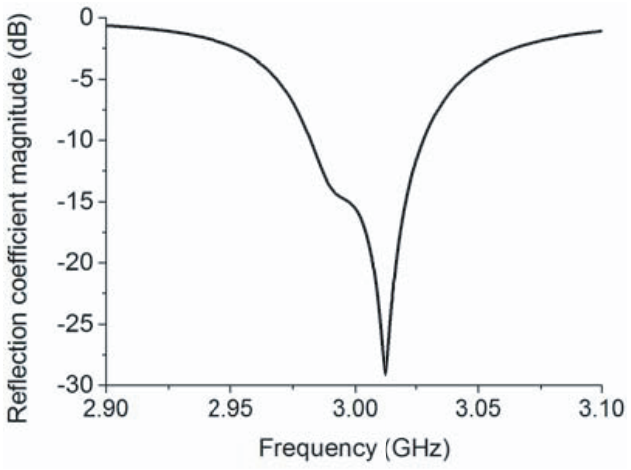

Figure 8. Simulated reflection coefficient magnitude of the radiating structure shown in Fig. 7 when the two elements are simultaneously excited.

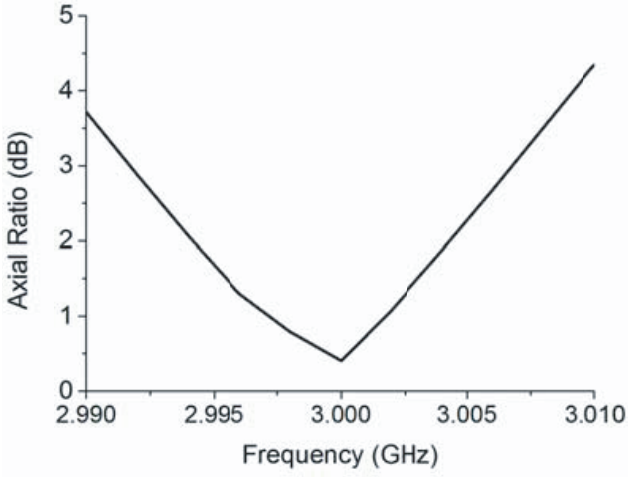

Figure 9. Simulated axial ratio in the main beam direction of the radiating structure shown in Fig. 7 when the two elements are simultaneously excited.

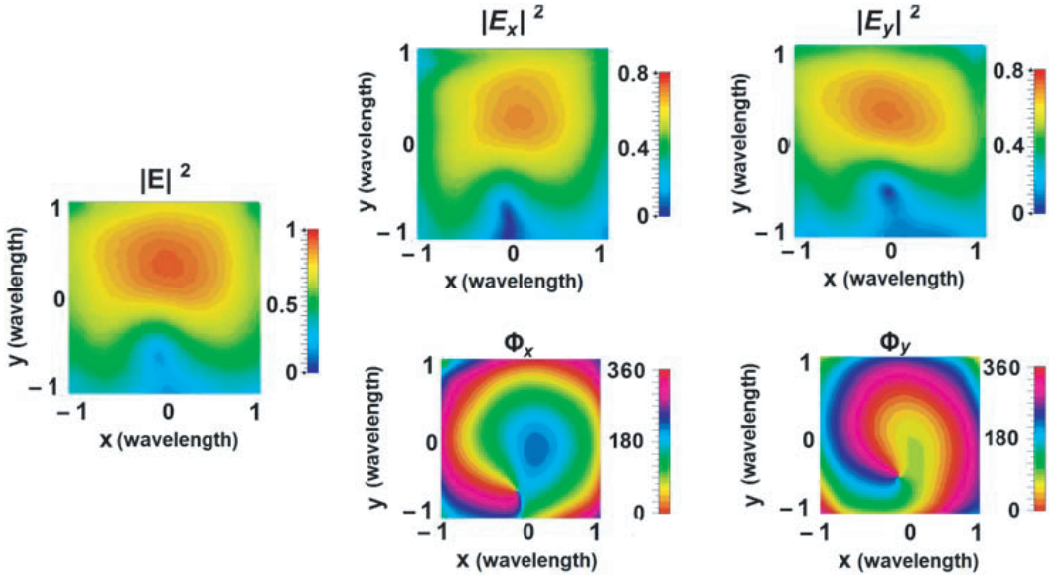

Figure 10. Numerically simulated total electric energy density ($|E|^2$), amplitude ($|E_x|^2$, $|E_y|^2$) and phase (Φ_x, Φ_y) distributions of the electric field radiated by the proposed structure when excited with both a RHCP TM_{11} and a RHCP TM_{21} modes for $\alpha = \pi/4$ and $\delta = 0$.

These patterns have the same shape as the corresponding ones reported in the previous Section, and confirm the possibility to exploit the phase singularity of vortex fields to enable new features in antenna systems.

Finally, in order to validate the possibility to shape and rotate the radiation pattern of the whole structure at will, we show in Figs. 11 and 12 the 3D radiation patterns for different values of α and δ, respectively. These patterns, which are in good agreement with the ones analytically calculated in the previous section, confirm that by varying α we can tailor the shape of the radiation pattern, while by varying δ we can change the main beam direction of the antenna. It is interesting that these knobs, easily controlled through the feeding network, can tailor the shape and directionality of radiation without affecting its topology, directly associated with the topological robustness of the proposed antenna.

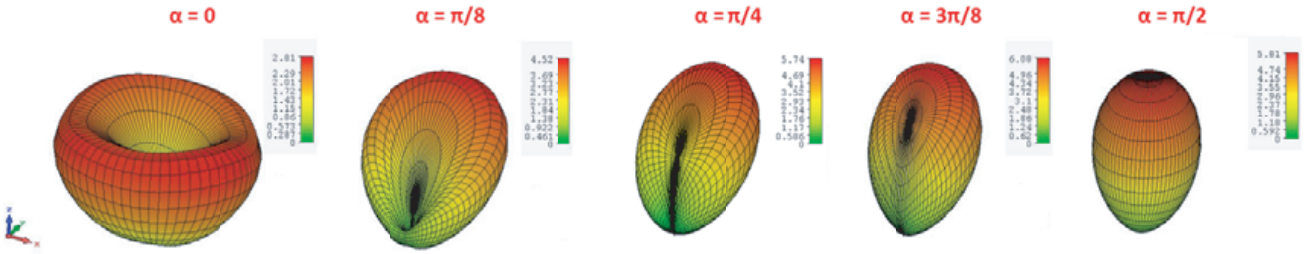

Figure 11. Numerically calculated gain patterns (expressed in dB) of the patch antenna supporting the superposition of RHCP TM_{11} and RHCP TM_{21} modes for different values of α.

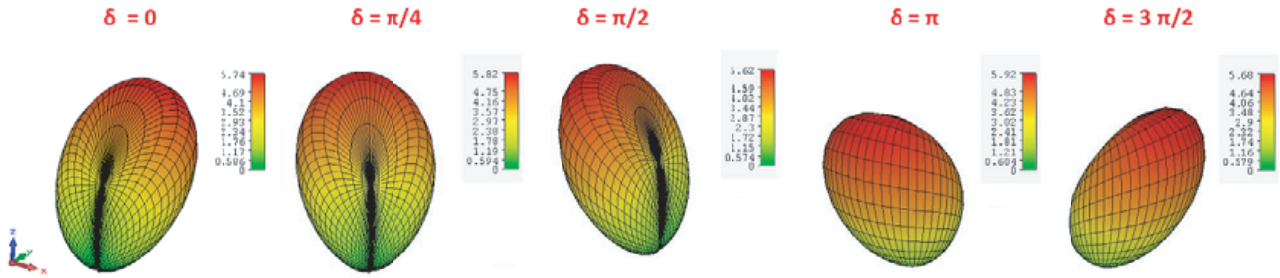

Figure 12. Numerically calculated gain patterns (expressed in dB) of the patch antenna supporting the superposition of a RHCP TM_{11} and a RHCP TM_{21} modes for different values of δ.

We remark here that since the '80, some studies have investigated the generation and superposition of different modes of radiating systems to manipulate the radiation pattern (see, for instance, [32–35]). However, our work allows establishing a direct link between the radiation performance of these systems and the topological properties of composite vortices. Moreover, this physical interpretation could be useful to further exploring applications of topology in radiation systems.

4. CONCLUSION

In summary, in this paper we have demonstrated that, by properly tailoring different modes of a patch antenna, we can tailor the complex field structures of composite vortices at microwave frequencies. In particular, by superimposing the first higher-order mode with the fundamental one of a circular patch antenna, we can translate and rotate at will the induced phase singularity of the first higher-order mode by simply changing the amplitude and/or phase of the excitation of the vortex-free fundamental mode. Moreover, as topological singularities have a direct impact on the radiation pattern of a radiating element, we have also shown that topological properties of composite vortices can be exploited to robustly shape and rotate the radiation pattern of a patch antenna. We have validated our approach performing a proper set of full-wave numerical simulations. Our results provide a reconfigurable and highly efficient way to generate vortices at microwave frequencies.

REFERENCES

1. Rubinsztein-Dunlop, H., et al., "Roadmap on structured light," *J. Opt.*, Vol. 19, 013001, 2017.
2. Nye, J. F. and M. V. Berry, "Dislocations in wave trains," *Proc. R. Soc. Lond. A*, Vol. 336, 165–190, 1974.
3. Soskin, M. S., V. N. Gorshkov, M. V. Vasnetsov, J. T. Malos, and N. R. Heckenberg, "Topological charge and angular momentum of light beams carrying optical vortices," *Phys. Rev. A*, Vol. 56, 4064–4075, 1997.

4. Grier, D. G., "A revolution in optical manipulation," *Nat.*, Vol. 424, 810-816, 2003.
5. Lee, J. H., G. Foo, E. G. Johnson, and G. A. Swartzlander, "Experimental verification of an optical vortex coronagraph," *Phys. Rev. Lett.*, Vol. 97, 053901, 2006.
6. Mair, A., A. Vaziri, G. Weihs, and A. Zeilinger, "Entanglement of the orbital angular momentum states of photons," *Nat.*, Vol. 412, 313–316, 2001.
7. Chen, R.-P., Z. Chen, Y. Gao, J. Ding, and S. He, "Flexible manipulation of the polarization conversions in a structured vector field in free space," *Laser Photonics Rev.*, Vol. 11, No. 6, 1700165, 2017.
8. Chen, R.-P., K.-H. Chew, C.-Q. Dai, and G. Zhou, "Optical spin-to-orbital angular momentum conversion in the near field of a highly nonparaxial optical field with hybrid states of polarization," *Phys. Rev. A*, Vol. 96, No. 5, 053862, 2017.
9. Chen, R.-P. and C.-Q. Dai, "Three-dimensional vector solitons and their stabilities in a Kerr medium with spatially inhomogeneous nonlinearity and transverse modulation," *Nonlinear Dyn*, Vol. 88, 2807–2816, 2017.
10. Chen, R.-P. and C.-Q. Dai, "Vortex solitons of the $(3+1)$-dimensional spatially modulated cubic-quintic nonlinear Schrödinger equation with the transverse modulation," *Nonlinear Dyn*, Vol. 90, 1563–1570, 2017.
11. Thide, B., H. Then, J. SjÄoholm, K. Palmer, J. Bergman, T. D. Carozzi, Y. N. Istomin, N. H. Ibragimov, and R. Khamitova, "Utilization of photon orbital angular momentum in the low-frequency radio domain," *Phys. Rev. Lett.*, Vol. 99, No. 8, 087701-1–087701-4, Aug. 2007.
12. Edfos, O. and A. J. Johansson, "Is orbital angular momentum (OAM) based radio communication an unexploited area?," *IEEE Trans. Antennas Propagat.*, Vol. 60, 1126–1131, 2012.
13. Mohammadi, S. M., L. K. S. Daldor®, J. E. S. Bergman, R. L. Karlsson, B. Thide, K. Forozesh, T. D. Carozzi, and B. Isham, "Orbital angular momentum in radio — A system study," *IEEE Trans. Antennas Propagat.*, Vol. 58, 565–572, 2010.
14. Tennant, A. and B. Allen, "Generation of OAM radio waves using circular time-switched array antenna," *Electron. Lett.*, Vol. 48, 1365–1366, 2012.
15. Tamburini, F., E. Mari, A. Sponselli, F. Romanato, B. Thidé, A. Bianchini, L. Palmieri, and C. G. Someda, "Encoding many channels in the same frequency through radio vorticity: First experimental test," *New J. Phys.*, Vol. 14, 033001, 2012.
16. Tamburini, F., E. Mari, B. Thidé, C. Barbieri, and F. Romanato, "Experimental verification of photon angular momentum and vorticity with radio techniques," *Appl. Phys. Lett.*, Vol. 99, 204102-1–204102-3, 2011.
17. Yu, S., G. Shi, C. Zhu, and Y. Shi, "Generating multiple orbital angular momentum vortex beams using a metasurface in radio frequency domain," *Appl. Phys. Lett.*, Vol. 108, No. 24, 241901, 2016.
18. Zhang, Z., S. Xiao, Y. Li, and B. Z. Wang, "A circularly polarized multimode patch antenna for the generation of multiple orbital angular momentum modes," *IEEE Antennas Wirel. Propag. Lett.*, Vol. 16, 521–524, 2017.
19. Hui, X., S. Zheng, Y. Hu, C. Xu, X. Jin, H. Chi, and X. Zhang, "Ultralow reflectivity spiral phase plate for generation of millimeter-wave OAM beam," *IEEE Antennas Wirel. Propag. Lett.*, Vol. 14, 966–969, 2015.
20. Mao, F., M. Huang, T. Li, J. Zhang, and C. Yang, "Broadband generation of orbital angular momentum carrying beams in RF regimes," *Progress In Electromagnetics Research*, Vol. 160, 19–27, 2017.
21. Barbuto, M., F. Trotta, F. Bilotti, and A. Toscano, "Circular polarized patch antenna generating orbital angular momentum," *Progress In Electromagnetics Research*, Vol. 148, 23–30, 2014.
22. Barbuto, M., F. Bilotti, and A. Toscano, "Patch antenna generating structured fields with a Möbius polarization state," *IEEE Antennas Wirel. Propag. Lett.*, Vol. 16, 1345–1348, 2017.
23. Bauer, T., P. Banzer, E. Karimi, S. Orlov, A. Rubano, L. Marrucci, E. Santamato, R. W. Boyd, and G. Leuchs, "Observation of optical polarization Möbius strips," *Science*, Vol. 347, 964–966, 2015.

24. Galvez, E. J., N. Smiley, and N. Fernandes, "Composite optical vortices formed by collinear Laguerre-Gauss beams," *Proceedings of SPIE 6131, Nanomanipulation with Light II*, 613105, Feb. 9, 2006.
25. Maleev, I. D. and G. A. Swartzlander, "Composite optical vortices," *J. Opt. Soc. Am. B*, Vol. 20, 1169–1176, 2003.
26. De Angelis, L., F. Alpeggiani, A. Di Falco, and L. Kuipers, "Persistence and fidelity of phase singularities in optical random waves," *Frontiers in Optics 2016, OSA Technical Digest (online) (Optical Society of America, 2016)*, paper JW4A.82, 2016.
27. Dennis, M. R., R. P. King, B. Jack, K. O'Holleran, and M. J. Padgett, "Isolated optical vortex knots," *Nature Physics*, Vol. 6, 118–121, 2010.
28. Flossmann, F., K. O'Holleran, M. R. Dennis, and M. J. Padgett, "Polarization singularities in 2D and 3D speckle fields," *Phys. Rev. Lett.*, Vol. 100, 203902, 2008.
29. Cardano, F., E. Karimi, L. Marrucci, C. de Lisio, and E. Santamato, "Generation and dynamics of optical beams with polarization singularities," *Opt. Express*, Vol. 21, 8815–8820, 2013.
30. Derneryd, A. G., "Analysis of the microstrip disk antenna element," *IEEE Trans. Antennas Propagat.*, Vol. 27, 660–664, 1979.
31. Huang, J., "Circularly polarized conical patterns from circular microstrip antennas," *IEEE Trans. Antennas Propagat.*, Vol. 32, 991–994, 1984.
32. Coleman, H. and B. Wright, "A compact flush-mounting antenna with direction finding and steerable cardioid pattern capability," *IEEE Trans. Antennas Propagat.*, Vol. 32, No. 4, 412–414, Apr. 1984.
33. Shafai, L., "Properties of microstrip phased arrays with self-scanning elements," *Digest on Antennas and Propagation Society International Symposium*, Vol. 2, 986–988, San Jose, CA, USA, 1989.
34. Lin, W., H. Wong, and R. W. Ziolkowski, "Wideband pattern-reconfigurable antenna with switchable broadside and conical beams," *IEEE Antennas Wirel. Propag. Lett.*, Vol. 16, 2638–2641, 2017.
35. Labadie, N. R., S. K. Sharma, and G. M. Rebeiz, "A circularly polarized multiple radiating mode microstrip antenna for satellite receive applications," *IEEE Trans. Antennas Propagat.*, Vol. 62, No. 7, 3490–3500, Jul. 2014.